

## EFFECT OF COLEMANITE AND PVA FIBRE IN ULTRA HIGH PERFORMANCE CONCRETE (UHPC) FOR RADIATION SHIELD

M. A. H. Abdullah\*<sup>1,2</sup>, R. S. M. Rashid<sup>1</sup>, Y. L. Voo<sup>3</sup>, N. M. Azreen<sup>4</sup>, H. Ithnin<sup>4</sup>  
and M. I. Idris<sup>6</sup>

<sup>1</sup> Department of Civil Engineering, Faculty of Engineering, Universiti Putra  
Malaysia, 43400 Serdang, Selangor, Malaysia.

<sup>2</sup> Department of Civil Engineering Technology, Faculty of Civil Eng. and  
Technology, University Malaysia Perlis, 02100 Perlis, Malaysia.

<sup>3</sup> DURA Technologies Sdn. Bhd, Jalan Chepor 11/8, Pusat Seramik Fasa  
2, Ulu Chepor, 31200 Chemor, Perak, Malaysia

<sup>4</sup> Bahagian Teknologi Industri, Agensi Nuklear Malaysia, 43600 Kajang,  
Selangor, Malaysia.

<sup>5</sup> School of Applied Physics, Faculty of Science and Technology, Universiti  
Kebangsaan Malaysia, 43600 Selangor, Malaysia.

\*corresponding: [afiqhizami@unimap.edu.my](mailto:afiqhizami@unimap.edu.my)

### Article history:

Received Date:

14 July 2023

Revised Date:

24 October 2023

Accepted Date:

5 January 2024

Keywords:

**Abstract**— Nuclear energy provides cleaner energy and detail imaging but due to its highly penetrative nature, shielding is required for safe handling. Concrete has been widely used and studied as shielding material but there is dearth on utilizing ultra-high-performance concrete (UHPC) especially on neutron radiation. This research aimed to investigate the effect of

UHPC, PHITS, Linear Attenuation Coefficient, Macroscopic Removal Cross Section, Heavyweight Aggregates	incorporating colemanite and polyvinyl alcohol (PVA) fibre in UHPC on its mechanical strength and radiation shielding. Compressive strength results show sand UHPdC with the highest value at 131 MPa. Magnetite and barite UHPdC recorded compressive strength of 118.7 and 116 MPa respectively. In terms of flexural and splitting tensile strength, sand UHPdC also recorded the highest value at 20.0 and 17.6 MPa respectively. However, the highest value of gamma radiation shielding is recorded by magnetite UHPdC at 0.1972 and 0.139 cm <sup>-1</sup> based on exposure to Cs-137 and Co-60 respectively while sand UHPdC recorded the lowest value. This is also shown in neutron shielding value as magnetite recorded the highest value at 0.0307 cm <sup>-1</sup> . Overall, presence of colemanite increase neutron shielding coefficient of UHPC but both colemanite and PVA fibre caused reduction in mechanical strength and gamma ray shielding of the concrete.
--	---

## I. Introduction

Harnessing of nuclear energy provides lots of benefits in healthcare, power generation and advancement in agriculture but the penetrative nature of its energy requires shielding which has been vastly made of concrete due to its ubiquitous components

and durability [1]–[5]. Familiarity of concrete as shielding for radiation is indicated by research that improves its radiation shielding properties via incorporation of beneficial element [6]–[8]. Vast study on radiation shielding concrete have been conducted

but there is a dearth of data involving ultra performance concrete as most of the research produced concrete with compressive and tensile strength of 49 MPa and 3 MPa [9]–[11].

Study also shows radiation shielding concrete possess low durability based on large mass loss due to sulfate attack [12]. Furthermore, thermal durability of radiation shielding concrete is low based on 30 and 90 % loss of strength and neutron shielding respectively when exposed to 500°C [13]. Further increase in temperature of 800°C resulted in 84.8 loss in compressive strength [14]. Utilization of ultra-high performance concrete (UHPC) which possess compressive strength of more than 120 MPa with superior thermal durability due to incorporation of fibre would provide nuclear related facility with better shielding [15]–[19].

Few research on UHPC as radiation shielding material shows compressive and flexural strength of more than 138 and 20 MPa respectively [7], [20], [21]. A research on magnetite UHPC shows residual

compressive strength of 23 MPa after exposure to 800°C [22]. However, there is lack of works on other type of heavyweight aggregate and incorporation with neutron absorbing mineral.

A combination of neutron absorbing element such as colemanite along with PVA fibre that helps improve concrete's thermal resiliency in composition of UHPC requires further investigation to assess its viability. Furthermore, there is also dearth of study on UHPC's neutron shielding performance which is beneficial for wider application in nuclear related facility. Hence, this study aimed to investigate the performance of UHPC with colemanite and polyvinyl alcohol (PVA) fibre in term of mechanical, radiation shielding that includes neutron shielding. This type of modified UHPC is denoted as ultra-high performance dense concrete (UHPdC).

## **II. Materials and Methods**

Ordinary Portland Cement type 1 is sourced from Tasek Corporation Berhad which follows MS EN 197-1:2014

guidelines. Three types of UHPdCs are produced that consist of fine-sized main aggregate that are either sand, barite or magnetite. Each main aggregate also is also combined with colemanite as neutron absorber. Sand used in sand UHPdC are sourced from river and sieved to three range of sizes; 0.65 – 300  $\mu\text{m}$ , 300 - 600  $\mu\text{m}$  and 0.6 – 1.18 mm. Barite are obtained from Minerals and Geoscience Department Malaysia which are sieved to sized less than 1.18 mm diameter. Magnetite is also sieved to less than 1.18 mm diameter that are sourced from

iron ore mine of Bestagold Sdn. Bhd. in Sungai Petani, Kedah. Colemanite are sourced from Turkey having powder-sized diameter.

Scanning Electron Microscope (SEM) images for magnetite, barite and colemanite is shown in Figure 1 based on 200  $\times$  magnification. Magnetite particles have cylindrical shape and larger in sized compared to barite. Barite particles are sized between 40 – 66  $\mu\text{m}$  but larger compared to colemanite. Only small population of colemanite having size between 22 – 40  $\mu\text{m}$  while the rest are sized between 12 – 22  $\mu\text{m}$ .

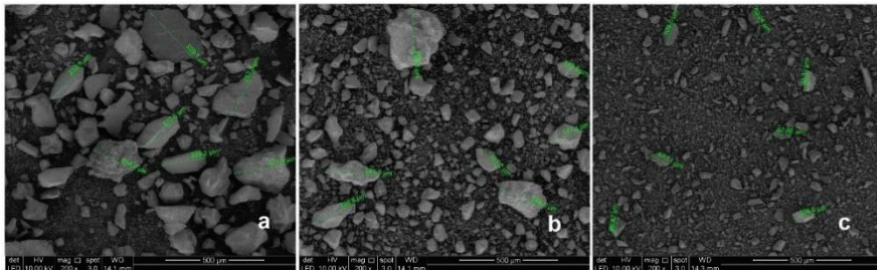


Figure 1: SEM analysis of a) magnetite, b) barite and c) colemanite at 200  $\times$  magnification

Two types of fibre used in this study are steel fibre and PVA fibre. Steel fibre is supplied by Ganzhou Daye Metallic Fibres Co., Ltd. with 20 mm length, 0.2

mm diameter and they are copper coated. Density of the steel fibre is 7840  $\text{kg}/\text{m}^3$  with 2850 MPa of tensile strength. PVA fibre used in this study is

0.015 mm in diameter, 12 mm in length with 1600 MPa of tensile strength. Density of fibre is 1300 kg/m<sup>3</sup>.

A total of three types of UHPdC are used in this study which are sand UHPdC, barite UHPdC and magnetite UHPdC

and 0.5 % by-volume of PVA fibre as shown in Table 1. Samples are mixed and tested for workability before moulded. Once hardened, samples are heat cured at 90°C for 48 hours and followed by air-cured for the remaining 24 days.

Table 1: Mix design for UHPdC

Sample	Cement (kg/m <sup>3</sup> )	Silica Fume (kg/m <sup>3</sup> )	Sand/ Barite/ Magnetite (kg/m <sup>3</sup> )	Colemanite (kg/m <sup>3</sup> )	PVA (kg/m <sup>3</sup> )	Super plasticizer (kg/m <sup>3</sup> )	Steel Fibre (kg/m <sup>3</sup> )	Water (kg/m <sup>3</sup> )
USS95 C5P0.5	825	200	950	50	9.75	28	120	191
UB95C 5P0.5	825	200	1580	50	9.75	28	120	226
UM95 C5P0.5	825	200	1819.3	50	9.75	28	120	236

Table 2: Physical properties of UHPdC

UHPdC	Workability (mm)	Density (kg/m <sup>3</sup> )	UPV (mm/s)
Sand UHPdC	170	2374±42	4640±18
Barite UHPdC	285	2776±16	4083±0
Magnetite UHPdC	215	2991±34	4348±0
Silica UHPC [22]	-	2424	-
Magnetite UHPC [22]	-	3339	-
M100 (barite concrete) [10]	-	2480	4149
M0 (sand concrete) [10]	-	2320	4615

A total of 9 nos. of 100 × 100 × 100 mm cubic samples, 12 nos of 100 × 100 × 500 mm prism samples and 9 nos. of 100 dia. × 200 mm cylinder are produced for this study which each type of

UHPdC is produced with triplicate sample for each type of dimension.

The workability of the mixes is determined using flow table apparatus. This is in accordance

with EN 1015-3. Hardened cubic samples are tested for Ultrasonic pulse velocity (UPV) test using direct method which is in accordance with BS EN 12504-4:2021. Tested samples are then tested for compressive strength based on BS EN 12390-3. Another type of sample which is cylindrical with 100 mm dia  $\times$  200 mm height is used for splitting tensile strength test based on BS EN 12390-6. Flexural strength is also determined based on BS EN 12350-5 using prism sample of 100  $\times$  100  $\times$  500 mm dimension.

For radiation shielding properties, prism samples of 100  $\times$  100  $\times$  20 mm that were cut from 100  $\times$  100  $\times$  500 mm prism block using concrete cutter were used in the test. The samples are air-dried before tested for gamma ray and neutron radiation shielding. Cs-137 (2 mCi) and Co-60 (1.14 mCi) are used as gamma radiation source for this study and these sources are detected with NaI scintillating detector. AmBe of 23.88 mCi activity was used as the source for neutron shielding and this is paired with Helium-3

neutron detector. A total of 8 slices of sample were tested for each type of UHPdC and the determination of radiation shielding property is based on Lambert's Law in linear attenuation coefficient ( $\mu$ ).

The coefficient is calculated based on the value of photon count,  $D$  after passing through sample with thickness,  $t$  and known photon count without sample,  $D_0$  as given in Equation (1). The  $\mu$  is estimated from trend of plotted data of  $\ln \frac{D_0}{D}$  against  $t$ . In term of macroscopic removal cross section,  $\Sigma_R(E_n)$ , the coefficient is calculated using the same principle and this is given in Equation (2).

$$\ln \frac{D_0}{D} = \mu t \quad (1)$$

$$\ln \frac{D_0}{D} = \Sigma_R(E_n)t \quad (2)$$

### III. Results and Discussion

Highest workability is recorded by barite UHPdC and this is followed by magnetite and sand UHPdC as shown in Table 2. This indicates that the finer the size of particles would result in higher workability as

sand UHPdC has coarsest particles among all UHPdCs. Coarser and more angular morphology of sand compared to other UHPdC led to larger friction between aggregate and fibre which leads to lower workability [23].

In term of density, UHPdC with heavyweight aggregate shows higher density compared to sand UHPdC. Magnetite UHPdC recorded the highest density at 2991 kg/m<sup>3</sup>. This is followed by barite and sand UHPdC. This is due to higher density of magnetite aggregate compared to other aggregate especially sand. A study comparing performance of silica UHPC with magnetite UHPC also shows similar trend with magnetite UHPC recorded UPV value at 37 % higher compared to silica UHPC. However, in term of quality of concrete structure, sand UHPdC recorded the highest value of UPV at 4640 mm/s. This is followed by magnetite and barite UHPdC. This indicates that sand UHPdC has more compactness in term of microstructural which is due to wider range of particle size

distribution. This is also shown in study of replacing sand with barite in concrete where sand concrete recorded larger UPV value compared to barite concrete [10].

### **A. Mechanical Properties**

Sand UHPdC recorded the highest compressive strength at 131 MPa and this is followed by magnetite and barite UHPdC as shown in Figure 2. This correlates with UPV value which indicates better microstructure resulted in better compressive strength of UHPdC. This is largely influenced by the wider range of particle size distribution and internal friction between particles due to morphology of sand.

Low compressive strength of barite UHPdC is also shown by study on UHPC that reported the similar trend [7]. Barite UHPC recorded the lowest compressive strength compared to silica and hematite UHPC. This may be due to high friability of barite aggregate based on Los Angeles abrasion test based on a study that compared it to limestone and slag [24]. In comparison to

other radiation shielding concrete, UHPdC recorded higher compressive strength as shown in Figure 2 which is due

to lower water-to-cement ratio [25]–[27].

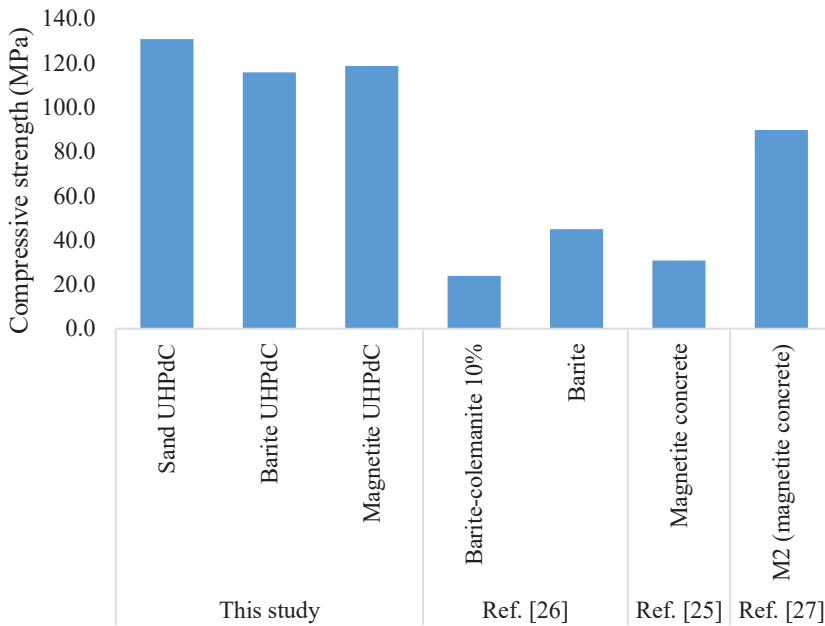


Figure 2: Graph of compressive strength (MPa) of different UHPdC and sample from previous studies

The presence of colemanite in concrete resulted in lower compressive strength yet strength of barite UHPdC which contained colemanite is still higher than barite-colemanite concrete from another study [26]. This is due to superior microstructural quality of UHPdC which reduced the negative effect of colemanite in concrete composition. Sand

UHPdC also recorded the highest value of flexural strength which is 20.0 MPa as shown in Figure 3.

This is higher compared to magnetite and barite UHPdC at 17.0 and 14.0 MPa respectively. This may be due to better compactness of sand UHPdC compared to other UHPdCs as indicated by UPV value. The compactness of matrix provides



better contact with steel fibre that is the crucial element in resisting flexural deformation. Furthermore, angular morphology of sand also provides better interlocking with steel fibre also led to higher flexural resistance.

Splitting tensile strength of UHPdCs also reflects the result of flexural strength. Sand

UHPdC recorded the highest value at 17.6 MPa while magnetite and barite UHPdC recorded the value at 15.2 and 14.4 MPa respectively. This further reinforces the superiority of sand UHPdC in terms of microstructural interaction between components of its composition compared to magnetite and barite UHPdC.

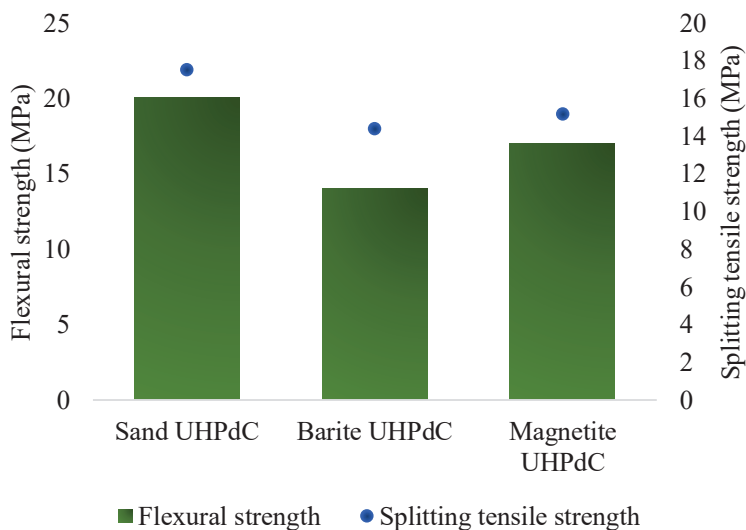


Figure 3: Flexural and splitting tensile strength of UHPdC

This is higher compared to magnetite and barite UHPdC at 17.0 and 14.0 MPa respectively. This may be due to better compactness of sand UHPdC compared to other UHPdCs as indicated by UPV value. The

compactness of matrix provides better contact with steel fibre that is the crucial element in resisting flexural deformation. Furthermore, angular morphology of sand also provides better interlocking with

steel fibre also led to higher flexural resistance.

Splitting tensile strength of UHPdCs also reflects the result of flexural strength. Sand UHPdC recorded the highest value at 17.6 MPa while magnetite and barite UHPdC recorded the value at 15.2 and 14.4 MPa respectively. This further reinforces the superiority of sand UHPdC in terms of microstructural interaction between components of its

composition compared to magnetite and barite UHPdC.

### B. Radiation Shielding

Result of gamma ray shielding shows denser UHPdC has higher shielding against gamma radiation. Based on exposure to Cs-137, magnetite UHPdC recorded highest  $\mu$  value at 0.1972; and this is followed by barite and sand UHPdC as shown in Figure 4. The trend is alike with source of Co-60.

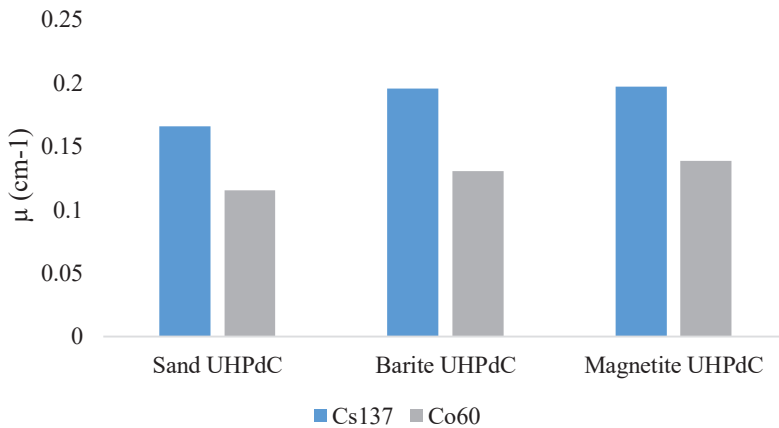


Figure 4: Graph of  $\mu$  ( $cm^{-1}$ ) value of various UHPdC

Magnetite recorded the highest value at  $0.139\text{ cm}^{-1}$  while barite and sand UHPdC recorded  $0.1306$  and  $0.1156\text{ cm}^{-1}$  respectively. This is largely influenced by heavy element presence in denser UHPdC

which is Fe and Ba in magnetite and barite UHPdC respectively. Sand UHPdC is less dense as it contains no heavy element.

Among heavyweight UHPdC, magnetite UHPdC shows higher gamma ray shielding compared

to barite UHPdC is due to higher percentage of Fe presence in magnetite aggregates compared to Ba in barite aggregates based on result of XRF. Overall, at higher energy of gamma source, the difference between shielding of UHPdC is reduced as the radiation is more penetrative. It is shown that the shielding coefficient of each UHPdC is lower compared to exposure to lower energy source.

In comparison to a study on UHPC as radiation shielding concrete, sand UHPdC recorded higher value of shielding coefficient which is  $0.1687 \text{ cm}^{-1}$  compared to  $0.146 \text{ cm}^{-1}$  the silica UHPC sample in the study that also contained PVA fibre [22]. This may be due to denser property of sand UHPdC compared to silica UHPC in the study. Another sample of the study which is magnetite UHPC recorded a similar  $\mu$  value with magnetite UHPdC at  $0.197 \text{ cm}^{-1}$  but amount of PVA fibre is lower in the UHPC. Overall, density of UHPdC largely

influences its gamma radiation shielding property.

The neutron shielding test used AmBe source which the result indicates higher neutron shielding coefficient is shown by denser UHPdC. Magnetite UHPdC recorded the highest  $\Sigma_R(E_n)$  value at  $0.0307 \text{ cm}^{-1}$  while barite and sand UHPdC recorded  $\Sigma_R(E_n)$  value at  $0.027$  and  $0.0262 \text{ cm}^{-1}$  respectively as shown in Figure 5. This is due to heavy elements in form  $\text{Fe}_2\text{O}_3$  and  $\text{Ba}_2\text{SO}_4$  in magnetite and barite respectively which contributed in moderating fast neutron by inelastic collision [28].

The moderated neutron is then absorbed by boron in colemanite which is a neutron absorber. This resulted in higher  $\Sigma_R(E_n)$  value hence higher shielding against neutron radiation. Magnetite UHPdC shows higher shielding compared to barite UHPdC as Fe in magnetite has higher absorption and scattering cross section compared to Ba in barite based on fast neutron [29]. This indicates that magnetite has higher chances of either absorbing or scattering a neutron

particle which resulted in better shielding.

In comparison to a study on dolomite concrete as dry cask storage, calculated neutron shielding value in the study is lower compared to the value

recorded by UHPdCs in this study [30]. The calculated value is based on absorption of thermal neutron of both dolomite concrete samples which are more than 0.4 % lower than magnetite UHPdC.

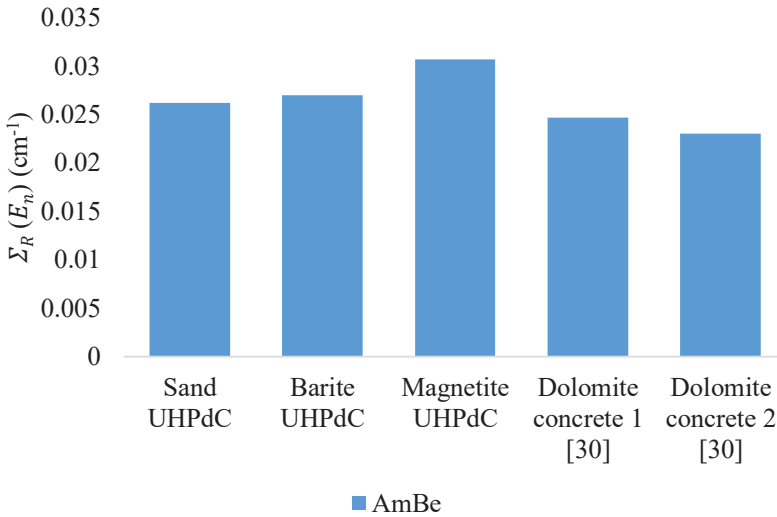


Figure 5: Graph of  $\Sigma_R(E_n)$  value of various UHPdC and dolomite concrete from previous study

#### IV. Conclusion

This study aimed to evaluate the performance of UHPdC in terms of mechanical and radiation shielding properties with the following conclusions are drawn:

Physical properties of sand UHPdC show better results compared to heavyweight UHPdC which are barite and

magnetite UHPdC. Mechanical properties of UHPdC largely correlated with physical properties as sand UHPdC shows better values. A wider range of particle sizes, sturdy aggregate and with more angular morphology resulted in higher mechanical strength of UHPdC. Gamma radiation shielding of UHPdC is largely influenced by

density as magnetite UHPdC recorded the highest value based on exposure to Cs-137 and Co-60. Neutron shielding based on AmBe source shows largest value recorded by magnetite UHPdC due to Fe element in the aggregate. Combination of element with large scattering cross section, neutron moderator and neutron absorber produced UHPdC with higher neutron radiation shielding property. Overall, magnetite UHPdC shows overall practical mechanical and highest shielding property.

From this study, it is shown that presence of colemanite and PVA fibre impacts negatively on gamma ray shielding and mechanical properties of UHPdC. However, the colemanite impacts positively on neutron shielding coefficient of the concrete and reducing effects from both colemanite and PVA fibre are minimized due to superior quality of UHPdC.

## V. References

- [1] N. A. Nordin, Z. Laili, and K. Samuding, "Persoalan tentang sinaran dan teknologi nuklear," *i-Nuklear*, 2019.
- [2] B. Baharuddin, H. Adnan, N. Mat Isa, N. P. bin M. Hasan, and S. S. Mat Sali, "MENANGANI COVID-19 : SUMBANGAN TEKNOLOGI NUKLEAR Sejarah Peranan," *i-Nuklear*, vol. 3, 2020.
- [3] G. R. CHOPPIN, J.-O. LILJENZIN, and J. RYDBERG, "Absorption of Nuclear Radiation," *Radiochem. Nucl. Chem.*, pp. 123–165, 2002, doi: 10.1016/b978-075067463-8/50006-6.
- [4] D. J. Naus, C. B. Oland, B. Ellingwood, Y. Mori, and E. G. Arndt, "Aging of concrete containment structures in nuclear power plants," p. 71, 1992, [Online]. Available: [http://inis.iaea.org/search/search.aspx?orig\\_q=RN:23071987](http://inis.iaea.org/search/search.aspx?orig_q=RN:23071987).
- [5] Centers for Disease Control and Prevention, "CDC Radiation Emergencies | Radioactive Contamination and Radiation Exposure." <https://www.cdc.gov/nceh/radiation/emergencies/contamination.htm>.
- [6] A. S. Ouda, "Development of high-performance heavy density concrete using different aggregates for gamma-ray shielding," *Prog. Nucl. Energy*, vol. 79, pp. 48–55, 2015, doi: 10.1016/j.pnucene.2014.11.009.
- [7] N. M. Azreen *et al.*, "Simulation of ultra-high-performance concrete mixed with hematite and barite aggregates using Monte Carlo for dry cask storage,"

- Constr. Build. Mater.*, vol. 263, p. 120161, 2020, doi: 10.1016/j.conbuildmat.2020.120161.
- [8] O. Lotfi-Omran, A. Sadrumontazi, and I. M. Nikbin, "A comprehensive study on the effect of water to cement ratio on the mechanical and radiation shielding properties of heavyweight concrete," *Constr. Build. Mater.*, vol. 229, 2019, doi: 10.1016/j.conbuildmat.2019.116905.
- [9] D. Mostofinejad, M. Reisi, and A. Shirani, "Mix design effective parameters on  $\gamma$ -ray attenuation coefficient and strength of normal and heavyweight concrete," *Constr. Build. Mater.*, vol. 28, no. 1, pp. 224–229, 2012, doi: 10.1016/j.conbuildmat.2011.08.043.
- [10] K. Saidani, L. Ajam, and M. Ben Oueddou, "Barite powder as sand substitution in concrete: Effect on some mechanical properties," *Constr. Build. Mater.*, vol. 95, pp. 287–295, 2015, doi: 10.1016/j.conbuildmat.2015.07.140.
- [11] S. H. Al-Tersawy, R. A. El-Sadany, and H. E. M. Sallam, "Experimental gamma-ray attenuation and theoretical optimization of barite concrete mixtures with nanomaterials against neutrons and gamma rays," *Constr. Build. Mater.*, vol. 289, p. 123190, 2021, doi: 10.1016/j.conbuildmat.2021.123190.
- [12] H. Binici, O. Aksogan, A. H. Sevinc, and A. Kucukonder, "Mechanical and radioactivity shielding performances of mortars made with colemanite, barite, ground basaltic pumice and ground blast furnace slag," *Constr. Build. Mater.*, vol. 50, pp. 177–183, 2014, doi: 10.1016/j.conbuildmat.2013.09.033.
- [13] S. Yousef, M. AlNassar, B. Naoom, S. Alhajali, and M. H. Kharita, "Heat effect on the shielding and strength properties of some local concretes," *Prog. Nucl. Energy*, vol. 50, no. 1, pp. 22–26, 2008, doi: 10.1016/j.pnucene.2007.10.003.
- [14] E. Horszczaruk and P. Brzozowski, "Investigation of gamma ray shielding efficiency and physicomechanical performances of heavyweight concrete subjected to high temperature," *Constr. Build. Mater.*, vol. 195, pp. 574–582, 2019, doi: 10.1016/j.conbuildmat.2018.09.113.
- [15] F. Zhang *et al.*, "Experimental study of CFDST columns infilled with UHPC under close-range blast loading," *Int. J. Impact Eng.*, vol. 93, pp. 184–195, 2016, doi: 10.1016/j.ijimpeng.2016.01.011.
- [16] P. Máca, R. Sovják, and P. Konvalinka, "Mix design of UHPFRC and its response to projectile impact," *Int. J. Impact Eng.*, vol. 63, pp. 158–163, 2014, doi: 10.1016/j.ijimpeng.2013.08.003.

- [17] J. Zhu, C. Sun, Z. Qian, and J. Chen, "The spalling strength of ultra-fiber reinforced cement mortar," *Eng. Fail. Anal.*, vol. 18, no. 7, pp. 1808–1817, 2011, doi: 10.1016/j.engfailanal.2011.05.001.
- [18] D. Zhang, Y. Zhang, A. Dasari, K. H. Tan, and Y. Weng, "Effect of spatial distribution of polymer fibers on preventing spalling of UHPC at high temperatures," *Cem. Concr. Res.*, vol. 140, no. November 2020, 2021, doi: 10.1016/j.cemconres.2020.106281.
- [19] D. Zhang and K. H. Tan, "Effect of various polymer fibers on spalling mitigation of ultra-high performance concrete at high temperature," *Cem. Concr. Compos.*, vol. 114, no. September, pp. 1–9, 2020, doi: 10.1016/j.cemconcomp.2020.103815.
- [20] N. M. Azreen, R. S. M. Rashid, M. Haniza, Y. L. Voo, and Y. H. Mugahed Amran, "Radiation shielding of ultra-high-performance concrete with silica sand, amang and lead glass," *Constr. Build. Mater.*, vol. 172, pp. 370–377, 2018, doi: 10.1016/j.conbuildmat.2018.03.243.
- [21] M. U. Khan, S. Ahmad, A. A. Naqvi, and H. J. Al-Gahtani, "Shielding performance of heavy-weight ultra-high-performance concrete against nuclear radiation," *Prog. Nucl. Energy*, vol. 130, no. October, p. 103550, Dec. 2020, doi: 10.1016/j.pnucene.2020.103550.
- [22] R. S. M. Rashid *et al.*, "Effect of elevated temperature to radiation shielding of ultra-high performance concrete with silica sand or magnetite," *Constr. Build. Mater.*, vol. 262, p. 120567, 2020, doi: 10.1016/j.conbuildmat.2020.120567.
- [23] S. L. Yang, S. G. Millard, M. N. Soutsos, S. J. Barnett, and T. T. Le, "Influence of aggregate and curing regime on the mechanical properties of ultra-high performance fibre reinforced concrete (UHPRFC)," *Constr. Build. Mater.*, vol. 23, no. 6, pp. 2291–2298, 2009, doi: 10.1016/j.conbuildmat.2008.11.012.
- [24] M. A. González-Ortega, S. H. P. Cavalaro, and A. Aguado, "Influence of barite aggregate friability on mixing process and mechanical properties of concrete," *Constr. Build. Mater.*, vol. 74, pp. 169–175, 2015, doi: 10.1016/j.conbuildmat.2014.10.040.
- [25] E. Horszczaruk, P. Sikora, and P. Zaporowski, "Mechanical properties of shielding concrete with magnetite aggregate subjected to high temperature," *Procedia Eng.*, vol. 108, pp. 39–46, 2015, doi: 10.1016/j.proeng.2015.06.117.
- [26] A. Mesbahi, G. Alizadeh, G. Seyed-Oskoei, and A. A.

- Azarpeyvand, “A new barite-colemanite concrete with lower neutron production in radiation therapy bunkers,” *Ann. Nucl. Energy*, vol. 51, pp. 107–111, 2013, doi: 10.1016/j.anucene.2012.07.039.
- [27] K. H. Yang, J. S. Mun, and H. J. Shim, “Shrinkage of heavyweight magnetite concrete with and without fly ash,” *Constr. Build. Mater.*, vol. 47, pp. 56–65, 2013, doi: 10.1016/j.conbuildmat.2013.05.034.
- [28] I. Akkurt and A. M. El-Khayatt, “The effect of barite proportion on neutron and gamma-ray shielding,” *Ann. Nucl. Energy*, vol. 51, pp. 5–9, 2013, doi: 10.1016/j.anucene.2012.08.026.
- [29] F. A. R. Schmidt, “Attenuation Properties Of Concrete For Shielding Of Neutrons Of Energy Less Than 15 Mev.,” *United States, 1970*. doi: 10.2172/4115490.
- [30] M. G. El-samrah, M. A. A. Zamora, D. R. Novog, and S. E. Chidiac, “Progress in Nuclear Energy Radiation shielding properties of modified concrete mixes and their suitability in dry storage cask,” *Prog. Nucl. Energy*, vol. 148, no. July 2021, p. 104195, 2022, doi: 10.1016/j.pnucene.2022.104195.